

## A novel method to synthesize nanocrystalline hydroxyapatite: Characterization with x-ray diffraction and infrared spectroscopy

Brahim Chafik El Idrissi<sup>a</sup>, Khalid Yamni<sup>b</sup>, Ahmed Yacoubi<sup>a</sup>, Asmae Massit<sup>a</sup>

<sup>a</sup>Equipe physique des surfaces et interfaces, Laboratoire de génie physique et environnement, Faculté des Sciences B.P 133, Kénitra, Université Ibn Tofail, Maroc.

<sup>b</sup>Equipe des Matériaux, Membranes et Procédés de Séparation. Faculté des Sciences Meknès, Université Moulay ismail. Maroc

---

**Abstract:** Hydroxyapatite  $\text{Ca}_{10}(\text{PO}_4)_6(\text{OH})_2$  (HA) is an important biomaterial and is the principal inorganic constituent of bones and teeth. It is also used as implant in the human body. By this investigation, hydroxyapatite nanostructured (18-56 nm) powders were prepared using novel wet precipitation method with calcium hydroxide and orthophosphoric acid solution as calcium and phosphorus precursors respectively. The Ca/P molar ratios of initial reagents are equal to 2.5. The HA filtered was dried at 90°C and calcined to different temperatures (300–1000°C). X-ray diffraction and Fourier transform infra-red spectroscopy used to characterize the calcined powder. The calcination reveals HA nano-powders. The particle size and crystallinity increase with the temperature. We note the formation of CaO at 1000°C. The refinement of cells parameters was performed by Fullprof-suite program. Thermal analysis (TG–DTA) was carried out to investigate the thermal stability of the powder.

**Key-Words:** hydroxyapatite, chemical precipitation, X-ray diffraction, FTIR, TG–DTA

---

### I. Introduction

Hydroxyapatite (HA) is one of most important market valued candidate biomaterial which is still in use since decades in medicine and dentistry applications. HA with chemical formula  $\text{Ca}_{10}(\text{PO}_4)_6(\text{OH})_2$ , assembling the main mineral components of bones and teeth, is among the leading biomaterials satisfying these requirements [1]. Synthetic HA has excellent biocompatibility due to its chemical stability with the mineral portions of hard tissues as well as its ability to constitute chemical bonding with surrounding tissues [2]. In medical and dental fields, the major application of this material is as bone graft, where HA is used to promote the growth of new bone. The successful growth of new bone tissue requires HA being biodegradable and bioresorbable. These characteristics are influenced by crystal size and crystallinity. The solubility of hydroxyapatite increases from crystalline to amorphous and with a reduction in crystal size. Many methods for synthesis of HA have been reported such as solid-state reaction, sol-gel, wet synthesis and hydrothermal methods. The keys factors for getting controllable aspect ratios and bioactivity are: the reaction temperature, the pH and the concentration of reactants. The properties of HA affect the efficiency of the powder in its ultimate applications [3]. All these properties of HA powders were depended on which process was performed. In particular, wet-chemical precipitation is the most complicated method [4, 5]. The wet-chemical precipitation was originally investigated by Jarcho and co-worker in 1976 [6]. Previously, the precursors of Ca and P are  $\text{Ca}(\text{NO}_3)_2 \cdot 4\text{H}_2\text{O}$  and  $(\text{NH}_4)_2\text{HPO}_4$  or  $(\text{NH}_4)\text{H}_2\text{PO}_4$  respectively [7, 8]. Only a few authors [9] selected  $\text{Ca}(\text{OH})_2$  and  $\text{H}_3\text{PO}_4$  as precursors. The correlation between the precipitation conditions and the properties of the powder was not found [10]. The disadvantages of the choice of the first series of precursors are the inevitability of rinsing several times with a greater amount of distilled water in order to eliminate the ammonium nitrate [11], and also, a greater amount of ammonia to make the  $\text{Ca}(\text{NO}_3)_2$  solution potently alkaline. Liou and al. [12] demonstrated that the activation energy of the  $\beta$ -TCP  $\text{Ca}_3(\text{PO}_4)_2$  (tricalcium phosphate) phase formation in systems with  $\text{H}_3\text{PO}_4$  as the P source was lower than those with  $(\text{NH}_4)\text{H}_2\text{PO}_4$ .

In this work Nano-size Hydroxyapatite powders were prepared by the wet chemical precipitation method but it is not a neutralization reaction. The calcium hydroxide and orthophosphoric acid solution are calcium and phosphorus precursors respectively. The Ca/P molar ratio of initial reagents is equal to 2.5. The use of this ratio means that the pH of the reaction mixture is self-buffered with high pH between 10 and 12. So we don't need the addition of any base such as ammonium hydroxide  $\text{NH}_4\text{OH}$  as reported in the literature.

However, the latter choice seems to be the most suitable because the only product is water [13].

The aim of the present study was to find the effect of sintering temperature on the crystallinity, crystallites size and phase composition of hydroxyapatite powders.

## II. Materials and methods

### 1. Powder synthesis

All of the powders were synthesized using a Ca/P molar ratio with the same value 2.5. The powders were prepared by conventional aqueous precipitation method. Briefly, orthophosphoric acid ( $\text{H}_3\text{PO}_4$ ) aqueous solution was added drop by drop (150  $\mu\text{l/s}$ ) into calcium hydroxide  $\text{Ca}(\text{OH})_2$  under-stirring aqueous suspension in all procedures. The purity of the starting materials was considered in the calculation of the concentrations of the solutions. The temperature of both the solution and the suspension dissolved in deionized water were controlled. The suspension was continuously stirred. After the total addition of the  $\text{H}_3\text{PO}_4$  solution, the pH remained greater than 10 (no ammonia was therefore added) and the suspension was continuously agitated for an additional 2 h at the same medium temperature and then matured over a period of 48 h at ambient temperature.

These matured suspensions were decanted and subjected to thermal treatment at 90°C for 24 h and ground to a fine powder in an agate mortar. The resulting oven-dried precipitates were calcined at a range of 300–1000°C in a dry air atmosphere using a ramp of 5°C/min with a soaking time of 1 h at peak temperatures, and then cooled in a furnace to ambient temperature at a cooling rate of 10°C/min.

### 2. Characterization

Crystalline phases were identified by means of a Shimadzu 6100 X-ray diffractometer (XRD) using  $\text{CuK}\alpha$  radiation and operating at 40 kV and 30 mA. XRD patterns were collected over the  $2\theta$  range of 10–60° at a step size of 0.02° and counting time of 0.5°/mn. Crystalline phases detected in the patterns were identified by comparison to standard patterns from the ICDD-PDF [14, 15]. Rietveld analysis was performed on the XRD of HA900 powder by using a Fullprof suite-2010 software program.

The functional groups present in the prepared powder calcined at 900°C were identified by FTIR (Vertex 70 Spectrometer). To perform a IR spectrum, 1% of the powder was mixed and ground with 99% KBr. Tablets of 10 mm diameter for FTIR measurements were prepared by pressing the powder mixture under 5 tons for 2 min and the spectrum was taken in the range of 400 to 4000  $\text{cm}^{-1}$  with resolution 4 and 128 times scanning. TG/DTA (Model Lapsys DSC-DTA/TG SETARAM) were performed in an air atmosphere only on the starting chemicals of our powder synthesis route over the range of 30°–1000°C, with a scan rate of 20°C/min. Transmission electron microscopy (TECNAI G2/FEI), operating at an accelerating voltage of 200 kV, was used to observe the powder morphology.

## III. Results and discussion

X-ray diffraction patterns of all HA samples treated at different temperature are shown in Figure 1 and Figure 2. The microstructure of the hydroxyapatite powders prepared by wet chemical precipitation method is strongly affected by the sintering temperature [14]. All XRD patterns shows diffraction peaks characteristics of hydroxyapatite presents in standards and in literature. The major phase, as expected, is hydroxyapatite, which is confirmed by comparing data obtained with the ICDD - PDF2 card: 00-009-0432. In case of sample heat treated at 90°C, XRD pattern revealed the presence of an important amorphous phase Figure 1.

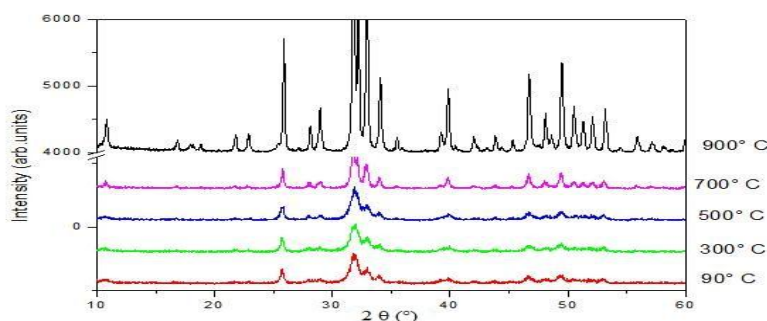


**Figure 1:** XRD spectra of dried and calcined HA powders.

The proportion of amorphous phase decreases with increasing of heat treatment temperature. XRD diffraction patterns of HAP-700, HAP-900 and HAP-1000 contain sharp peaks and exactly match the crystalline of HA. Also the diffraction peaks (002), (211), (112) and (300) planes are intensified with the increase of calcining temperature. It should be noted that the widths of the peaks become more narrow indicating an increase in the crystallinity of HA powders. XRD patterns of powders showed no presence of secondary phases indicating that the final product was of high purity. Beside the hydroxylapatite, a small amount of CaO was identified in the powder treated at 1000°C (HA1000) identified at 37.35 and 53.85 ( $2\theta$ ) Figure 2.

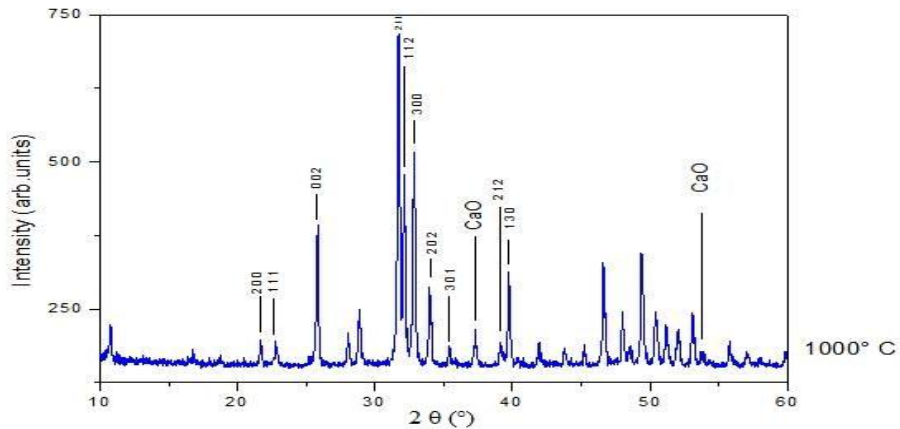


**Figure 2:** XRD spectrum of calcined HA at 1000°C

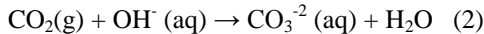
The presence of CaO after heat treatment is in agreement with the results reported by Kutty [15], Skinner [16] and A. Costescu [17]. With the increase of the calcination temperature HA would have started losing hydroxyl groups forming various phosphates. The proposed reaction is [14]:



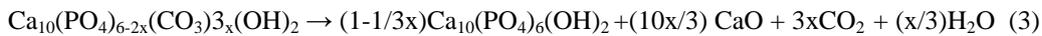
The presence of CaO in hydroxyapatite ceramics, designed for medical applications cannot be accepted. In contact with water molecules CaO, if is present in ceramic, converts into calcium hydroxide. That results in gradual tension and hair cracks in the ceramic material. The swelling and the disintegration into individual particles can also generate strong alkalinity in the implant environment [18].

The  $\text{Ca}_3(\text{PO}_4)_2$  phase cannot be seen in the XRD pattern of the sample annealed at 1000°C. The presence of the  $\beta\text{-Ca}_3(\text{PO}_4)_2$  can be detected only by the slight shoulder on the left hand side of HA (211). In our case, we have not a  $\beta$  tricalcic phosphate.

The  $\text{CO}_3^{2-}$  ions possibly penetrated the low crystallinity HA as a common contaminant from the atmosphere during the precipitation process, because the reactor was freely exposed to air in the present experiment and small part of the  $\text{PO}_4$  (B-type) groups in the apatitic structure was replaced by  $\text{CO}_3$ . The dissolution of carbon dioxide from the atmosphere occurs by the following reaction:



It has been established that at elevated temperatures carbonate groups are decomposed. As a result  $\text{CO}_2$  has been emitted and free calcium oxide CaO has been formed [19]:



In order to obtain a pure HA in this study, the calcining temperature selected should be below the temperature of 1000°C. As shown in Figure 3.

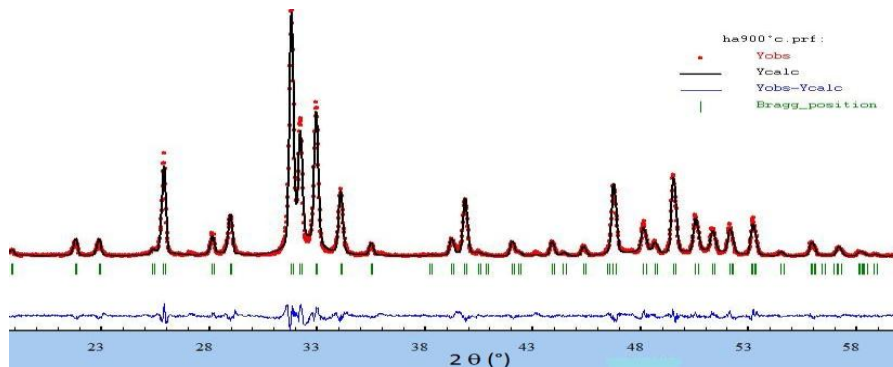


**Figure 3:** Rietveld analysis of HA900 powders

XRD peaks indicating a pure powder. Lattice dimensions (a-, b- and c-axis dimensions) were calculated for the fitted peaks. They were determined as  $a = 0.94137$  nm,  $b = 0.94137$  nm and  $c = 0.68809$  nm with angles  $\alpha = \beta = 90^\circ$  and  $\gamma = 120^\circ$ , with space group  $P6_3/m$  indicating a hexagonal unit cell structure. The experimental parameters are in good agreement with those reported as standard values ( $a = b = 0.94160$  and  $c = 0.68830$  nm).

The mean crystallite size (L) of the particles was calculated from the XRD line broadening measurement using the Scherrer equation (1) [19]:

$$L = 0.89 \lambda / \beta \cos\theta \quad (1)$$

Where L is the mean dimension of the homogeneous crystallites along an axis perpendicular to the hkl system considered,  $\beta$  (in radians) is the width at half maximum, K is the Scherrer constant approximation close to 0.89,  $\lambda$  is the corresponding X-ray wavelength,  $\theta$  is the position of the peak in degrees. In the case of HAP, the Scherrer equation is relative to a single peak (211).

An estimation to crystallites size for hydroxyapatite powders, according to Scherrer's formula reveals a proportional increase of crystallite size from 18 nm to 56 nm with increasing of the heat treatment temperature from 90 – 1000°C. The estimated crystallites size of hydroxyapatite are in according with data obtained regarding the crystallinity degree.

The fraction of crystalline phase ( $X_c$ ) of the HA powders was evaluated by the following equation, Eq. (2) [20]:

$$X_c = 1 - v_{112/300} / I_{300} \quad (2)$$

Where  $I_{300}$  is the intensity of (3 0 0) diffraction peak and  $v_{112/300}$  is the intensity of the hollow between (112) and (3 0 0) diffraction peaks of HA.

The crystallinity degree increases from 35% to 94% the heat treatment temperatures from 90°C to 1000°C. It could be observed that both the crystallite size and crystallinity increase with the calcination temperature. FTIR patterns presented in Figure 4. confirm the formation of HA calcined at 900°C.

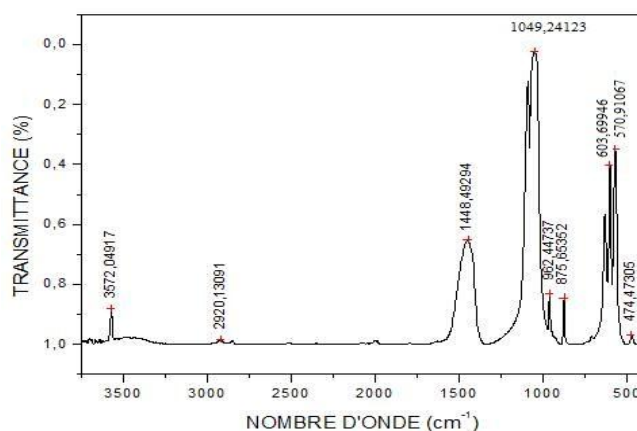


**Figure 4:** IR spectrum of HA900 powder.

FTIR spectrum of HA contains characteristic phosphate, carbonate and hydroxyl bands. Phosphate bands are:  $\nu_3$  band in the region 1092–1048  $\text{cm}^{-1}$  corresponding to triply degenerated anti-symmetric P–O stretching,  $\nu_1$  band at 963  $\text{cm}^{-1}$  corresponding to non-degenerate symmetric P–O stretching,  $\nu_4$  bands at 603 and 571  $\text{cm}^{-1}$  corresponding to triply degenerated O–P–O bending and  $\nu_2$  band at 474  $\text{cm}^{-1}$  assigned to the components of doubly degenerate O–P–O bending mode. Bands in the region 1650–1300  $\text{cm}^{-1}$  and at 872  $\text{cm}^{-1}$  are carbonate  $\nu_3$  and  $\nu_2$  bands, respectively. Sharp bands at 3573  $\text{cm}^{-1}$  and 633  $\text{cm}^{-1}$  correspond to stretching and librational modes of hydroxyl vibrations, respectively.

The DTA and TGA curves for the hydroxyapatite powder after drying are illustrated in Figure 5, we can see two endothermic peaks at 97°C and 185°C which correspond to the loss physically of absorbed water molecules and the removal of crystallized water. The weight loss is about 7.5 % by weight, with increasing temperature from 400 to 620°C no significant wt. loss was observed and no peak has been detected, except an exothermic peak is observed at the DTA curve at 450°C could be due to a crystallization process of the powder.

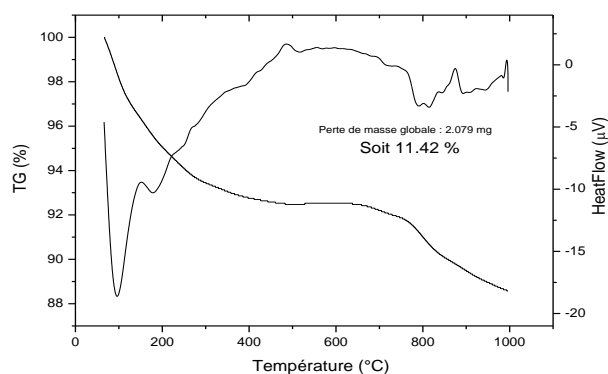
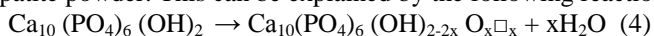
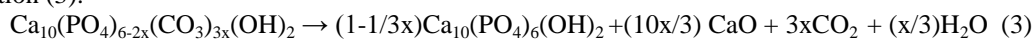


**Figure 5:** DTA and TG curves of the gel dried at 90°C

The weight loss of 2% between 600 and 800°C is assumed to be resulted gradual dehydroxylin of the hydroxyapatite powder. This can be explained by the following reaction (4):



In temperature between 800°C and 1000°C, there is a small exothermic peak along with 1.9% weight loss, the slight decrease in TGA curves shows the decomposition of  $\text{Ca}_{10}(\text{PO}_4)_{6-2x}(\text{CO}_3)_{3x}(\text{OH})_2$  in CaO,  $\text{CO}_2$  and  $\text{H}_2\text{O}$  by the reaction (3):



This result is in good agreement with the occurrence of CaO lines in the XRD patterns at 1000°C.

The TEM micrograph of HA calcined at 900°C is shown in Figure 6. It reveals that the sample present a rod-like morphology with sizes about 30-50 nm in the short axis and 70-180 nm in the long axis.

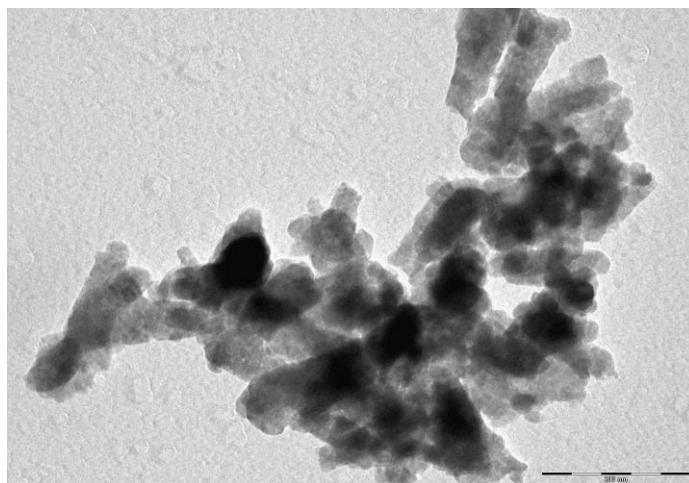


**Figure 6:** TEM images of HA calcined at 900°C.

The growth of hydroxyapatite rods usually occurs along the c-axis [25]. It can also be seen that the calcined powder exhibited high tendency to agglomerate.

#### IV. Conclusion

The novel method for the synthesis of hydroxyapatite powders led to obtaining a product with a high degree of crystallinity and purity. The crystallinity degree was greater than 94%. The X – ray diffraction analysis reveal the presence of insignificant amounts of calcium oxide as secondary phase identified in the powder treated at 1000°C. Rietveld analysis also revealed high purity and the dimensions of the unit cell of calcined HA, indicating a hexagonal structure. The IR spectrum confirms the formation of hydroxyapatite and suggest the presence of  $\text{CO}_3^{2-}$  in hydroxyapatite structure. In order to obtain pure HA in this study, the temperature selected for calcination should be below 1000°C.

## References

- [1] N. Demirkol, E.S. Kayali, M. Yetmez, F.N. Oktar, S. Agathopoulos, *Key Eng. Mater.* 484, 204 (2011).
- [2] S. Ramesh, P. Christopher, C.Y. Tan, W.D. Teng, *Biomed. Eng.-Appl. Basis Commun.* 16, 199 (2004).
- [3] Chandrasekhar Kothapalli, M. Wei, A. Vasiliev, M.T. Shaw, *Acta Materialia* 52, 5655 (2004).
- [4] Cao, L., Zhang, C. and Huang, J. 2005. Synthesis of hydroxyapatite nanoparticles in ultrasonic precipitation. *Ceram. Int.* 31 : 1041-1044.
- [5] Kong, L.B., Ma, J. and Boey, F. 2002. Nano- sized hydroxyapatite powders derived from coprecipitation process. *J. Mater. Sci.* 37 : 1131-1134.
- [6] Jarcho, M. and Bolen, C.H. 1976. Hydroxyapatite synthesis and characterization in dense polycrystalline form. *J. Mater. Sci.* 11 : 2027-2035
- [7] H. Liu, H. Yazici, C. Ergun, T.J. Webster, H. Bermek, An in vitro evaluation of the Ca/P ratio for the cytocompatibility of nano-to-micron particulate calcium phosphates for bone regeneration, *Acta Biomaterialia* 4 (2008) 1472–1479.
- [8] M. Descamps, J.C. Hornez, A. Leriche, Effects of powder stoichiometry on the sintering of [beta]-tricalcium phosphate, *Journal of the European Ceramic Society* 27 (2007) 2401–2406.
- [9] A. S ´Alósarczyk, E. Stobierska, Z. Paszkiewicz, M. Gawlicki, Calcium phosphate materials prepared from precipitates with various calcium: phosphorus molar ratios, *Journal of the American Ceramic Society* 79 (1996) 2539–2544.
- [10] A. Osaka, Y. Miura, K. Takeuchi, M. Asada, K. Takahashi, Calcium apatite prepared from calcium hydroxide and orthophosphoric acid, *Journal of Materials Science: Materials in Medicine* 2 (1991) 51–55.
- [11] F.-H. Lin, C.-J. Liao, K.-S. Chen, J.-S. Sun, Preparation of high-temperature stabilized [beta]-tricalcium phosphate by heating deficient hydroxyapatite with Na<sub>4</sub>P<sub>2</sub>O<sub>7</sub> ·10H<sub>2</sub>O addition, *Biomaterials* 19 (1998) 1101–1107.
- [12] S.-C. Liou, S.-Y. Chen, Transformation mechanism of different chemically precipitated apatitic precursors into [beta]-tricalcium phosphate upon calcination, *Biomaterials* 23 (2002) 4541–4547.
- [13] A. Osaka, Y. Miura, K. Takeuchi, M. Asada, K. Takahashi, Calcium apatite prepared from calcium hydroxide and orthophosphoric acid, *Journal of Materials Science: Materials in Medicine* 2 (1991) 51–55.
- [14] M. Sivakumar, T.S.S. Kumart, K.L. Shantha, K.P. Rao, Development of hydroxyapatite, derived from Indian coral, *Biomaterials* 17 (1996) 1709–1714.
- [15] M.N. Salimi, R.H. Bridson, L.M. Grover, G.A. Leeke, Effect of processing conditions on the formation of hydroxyapatite nanoparticles, *Powder Technol.* 218 (2012) 109–118.
- [16] D. Predoi, R.A. Vatasescu-Balcan, I. Pasuk, R. Trusca, M. Costache, *Journal of Optoelectronics and Advanced Materials*, 10(8), 2151 (2008)
- [17] T.R.N. Kutty, *Indian J. Chem.* 11, 695 (1973)
- [18] H.C.W. Skinner, J.S. Kittelbergen, R.A. Beebe, *J. Phys. Chem.* 79, 2017 (1975)
- [19] A. Costescu, I. Pasuk, F. Ungureanu, A. Dinischiotu, M. Costache, F. Huneau, S. Galaup, P. Le Coustumer, D. Predoi, *Digest Journal of Nanomaterials and Biostructures*, 2010, 989-1000.
- [20] B.S. Haibo Wang, Hydroxyapatite degradation and biocompatibility, dissertation, The Ohio State University, 2004.
- [21] H. El Feki, I. Khattech, M. Jemal, C. Rey., Décomposition thermique d'hydroxyapatite carbonates sodées. *Thermochemica Acta*, Vol.237, 1994, p. 99-110
- [22]. H.P. Klug, L.E. Alexander, *X-ray diffraction procedures for polycrystalline and amorphous materials*, Wiley Interscience, London, 1974, p. 656-690.
- [23] Landi, E., Tampieri, A., Celotti, G., & Sprio, S. (2000). Densification behaviour and mechanisms of synthetic hydroxyapatites. *Journal of the European Ceramic Society*, 20, 2377–2387.
- [24] I. Mobasherpour, M. Soulati Heshajin, A. Kasemzadeh, M. Zakiri, *Journal of alloys and compounds* 430 (2007) 330-333.
- [25] I. S. Neira, Y. V. Kolen'ko, O. I. Lebedev, G. Van Tendeloo, H. S. Gupta, F. Guitián, M. Yoshimura, *Cryst Growth Des.* 9, 466 (2009).